Automation in Construction 19 (2010) 742–749

Contents lists available at ScienceDirect

Automation in Construction

journal homepage: www.elsevier.com/locate/autcon

Measuring building façades with a low-cost close-range photogrammetry system

Celestino Ordóñez *, Joaquín Martínez, Pedro Arias, Julia Armesto

Mining School, Rua Maxwell s/n, University of Vigo, 36310 Vigo, Spain

ARTICLE INFO

Article history:
Accepted 10 March 2010

Keywords:
Close-range photogrammetry
Laser distance meter
Calibration
Precision
Façade measurement

ABSTRACT

The dimensions of façades and window openings are usually determined by direct measurements using tapes and plummets. These direct methods are time consuming and risky for operators, so indirect approaches are needed. In this paper, we analyse a planar-surface measuring system based on close-range photogrammetry to determine its accuracy and precision. This system is composed of a digital camera and a laser distance meter mounted on a support that allows the laser distance meter to be moved independently of the camera. The proposed system can determine the dimensions of objects. Also, this system provides an estimation of the precision of the calculations for the distances between points. By knowing the uncertainty of their measurements, users can accept or reject the measurement depending on the application tolerance.

1. Introduction

Photogrammetry is the technique of measuring objects from images. One of the features of photogrammetry is that the measurements are usually taken without any contact with the object to be measured. With the increasing quality and decreasing prices of digital photography, low-cost close-range photogrammetry has become more popular, and software applications have been developed that can provide photogrammetry to non-specialised users. Photogrammetric projects based on photographs consist of obtaining a 3D model that makes it possible to make measurements of an object. These 3D models can be composed of different types of objects. The process for obtaining such a 3D model consists of orienting the photographs, referencing points in two or more oriented images and reconstructing the 3D model by math intersection.

It is possible to solve the 3D model from a single-image; the key is that it is necessary to provide additional information such as geometric constraints. In [1], two sets of constraints are described: object constraints and topology constraints; applying more constraints than needed leads to an adjustment process. The object constraints include parallelism, perpendicularity and symmetry. The topology constraints are planar (coplanarity), linear and point constraints. A line constraint is widely used. The same author in [2] described the use of coplanar parallel lines to determine the exterior orientation of an object. The orientation is achieved in two steps using parallelism information in the first step and introducing at least seven object coordinates in order to determine the exterior orientation in the second step. Before this technique was developed, several authors had used line constraints [3]. In [4], a method for 3D reconstruction using collinearity, perpendicularity and parallelism constraints provided by the user is presented. In that work, vanishing points are computed as the intersection of sets of images of parallel 3D line segments. Vanishing points are widely used for camera calibration, as described in [5,6], as well as in single-image 3D reconstruction [7,8]. In [9] some new methods for vanishing point detection are presented. These methods were used in [10] to find a metric reconstruction from single images.

In [10,11], the metric reconstruction of the façades of damaged or destroyed historical buildings using historical single-view photographs is presented. In [12], a camera is used as a plane measuring device, and in [13] the authors describe how to obtain 3D measurements as well as uncertainties from a single perspective view. The authors in [3] propose a method for single-image measurements used for determining the dimensions of flat surfaces such as billboards. Image orientation is achieved through horizontal and vertical lines and the scale of the image is determined from the distance read by a laser distance meter parallel to the optical axis. In [14], the authors proposed an improvement to the method described in [3], permitting relative rotations between the laser distance meter and the digital camera, a technique that was applied to measurements of façade window apertures. The particular orientation is based on the vanishing line of the reference plane of the façade and scaling is achieved with a laser distance meter.

This work is a continuation of [14] where a method for determining the precision of photogrammetry measurements, based on the propagation of uncertainties in the measurement process, is proposed. Also, we introduce some changes on the orientation and scaling procedures and also on the calculation of vanishing points in order to achieve more accurate measurements.

* Corresponding author. E.T.S.I.MINAS, Rua Maxwell s/n, Campus Lagoas-Marcosende, Universidad de Vigo, 36310 Vigo, Spain. Tel.: +34 986814052; fax: +34 986811924.
E-mail addresses: cgalan@uvigo.es (C. Ordóñez), joaquin.martinez.sanchez@gmail.com (J. Martínez), parias@uvigo.es (P. Arias), julia@uvigo.es (J. Armesto).

0926-5805/$ – see front matter © 2010 Elsevier B.V. All rights reserved.
doi:10.1016/j.autcon.2010.03.002

2. Measurement system

The measurement system consists of three elements: a digital camera, a laser distance meter and a specifically designed support for these two devices. A more detailed description of the measurement system can be found in [14]. The support was built out of aluminium, except for rotating wheels that were made of steel. Fig. 1 shows a view of the system. This system makes it possible to set the distance from the optical centre of the digital camera to the object we want to measure based on the triangulation principle. This distance determines the scale of pixel measurements and object-space measurements if the image is properly oriented to the object.

2.1. System calibration

In order to use this system, we must first calibrate it. In [3], this type of system is calibrated and the calibration process establishes the camera parameters and the distance meter eccentricity at the same time. In this work, each component of the system is calibrated independently: the camera, the distance meter and the support. The camera calibration was performed by the well-known software *Photomodeler* [15]. The calibration procedure consists of taking several camera shots in a calibration grid in different positions and orientations. These photographs are oriented in an adjustment process that is known as an interior orientation of the camera, which is used to determine the camera's pinhole model parameters. These parameters include the focal length, the principal point position and the lens distortion parameters. The laser distance meter is calibrated by the vendor and is stable during the measurement process. To calibrate the support we note that the measurement system is based on the triangulation principle, so we need to know the following:

- the distance meter's centre position vector referred to camera's optical centre:

$$\vec{L} = (X_L - X_0, Y_L - Y_0, Z_L - Z_0)^T \quad (1)$$

- the unitary direction vector of the distance meter laser beam in relation to the camera's orientation:

$$\vec{V} = \left(V_x, V_y, V_z\right)^T \quad (2)$$

Determining the support parameters consists of taking some shots at the distance meter laser pointer at several distances, so the wavelength of the laser needs to be in the visible spectrum. For every single shot, we can establish the following relation

$$\vec{L} + d\cdot\vec{V} = \vec{X}_{LP} \quad (3)$$

Fig. 1. View of the measuring system with their different elements: laser distancemeter, digital camera and aluminium support.

where L and V are the distance meter position and direction vectors, respectively, d is the distance from the distance meter to the laser pointer and X_{LP} is a vector that contains the laser pointer object coordinates

$$\vec{X}_{LP} = (X_{LP} - X_0, Y_{LP} - Y_0, Z_{LP} - Z_0)^T, \quad (4)$$

where the subscript *LP* stands for the laser pointer's coordinates and the coordinates with a subscript 0 refer to camera's optical centre coordinates. In Fig. 2 the triangle constructed to calibrate the support is represented. As it can be seen, the origin of the reference system is located on the optical centre of the camera.

To obtain the relationship between the object and image coordinates, we use the collinearity property

$$\vec{X}_{LP} = k\cdot R\cdot\vec{x}_{LP} \quad (5)$$

where

- X_{LP} are the object coordinates of the distance meter laser pointer,
- k is the scale factor between object and image coordinate spaces,
- R is the rotation matrix between object and image coordinate systems
- x_{LP} are the image coordinates of the distance meter laser pointer:

$$\vec{x}_{LP} = (x_{LP} - x_0, y_{LP} - y_0, -c - z_0)^T \quad (6)$$

and c is the camera's focal length.

Assuming both of the coordinate systems' centres $X_0 = x_0 = (0,0,0)^T$ and $R = I$ the identity matrix, the relationship between the object and image coordinates can be rewritten as:

$$(X_L, Y_L, Z_L)^T + d\cdot(V_X, V_Y, V_Z)^T = k(x_L P, y_L P, -c)^T \quad (7)$$

where d, x_{LP}, x_{LP} and c are known. Using the restriction given by $\|\vec{V}\| = 1$, we have a three-equation system with six unknowns, five unknowns in support parameters and the scale factor k, for every image. If we take at least three images, we form an over-determined system that can be solved using the least squares method (LSM). In this way we can obtain the value and the precision of the parameters that model the support. Fig. 3 shows different shots of the calibration process.

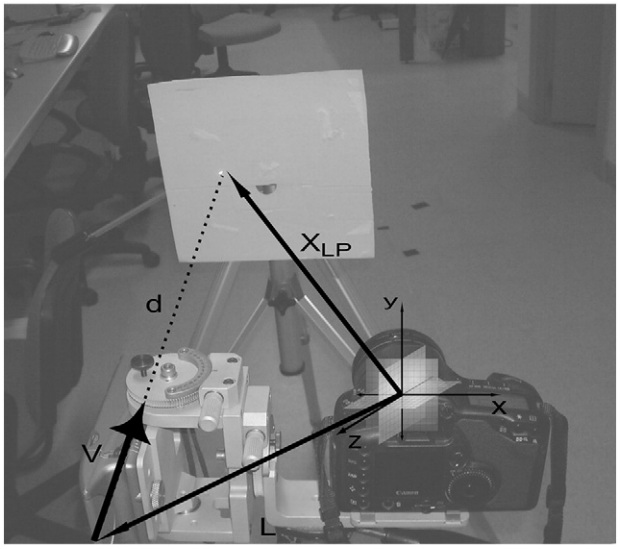

Fig. 2. Representation of the triangulation procedure used to calibrate the support.

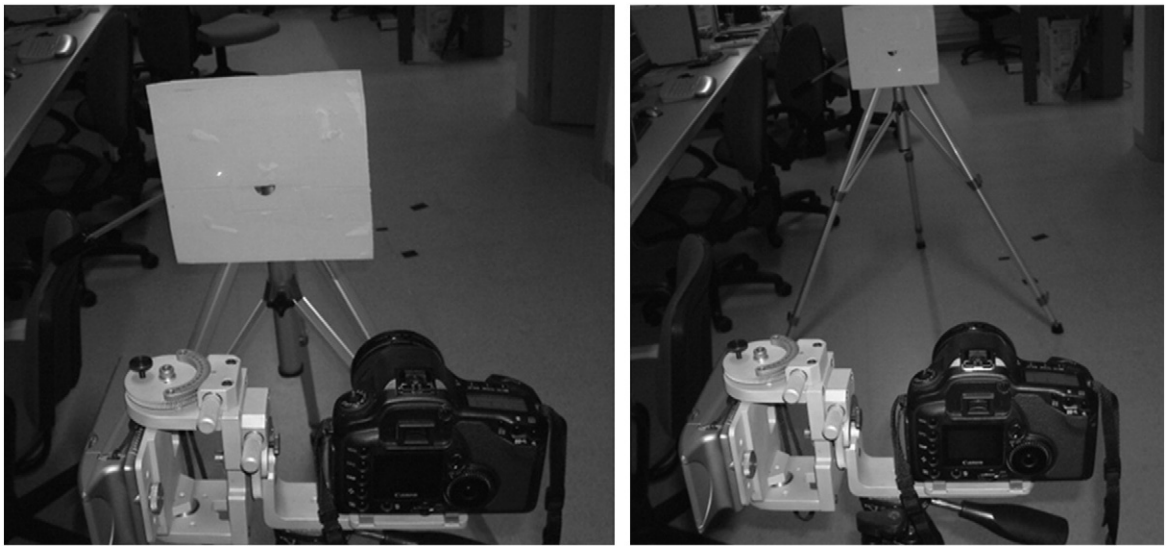

Fig. 3. Calibration methodology. The pictures show the method used to calibrate the system. The shots are taken at different distances.

2.2. Measurement system method

In order to make measurements in a 3D space from photographs, it is necessary to know the exterior orientation of every image and the scale factor between the oriented image coordinates and object's real world coordinates. In case of single-image orientation, we need to apply constrains to the image [1–4].

2.2.1. Image orientation

In this work, the image orientation is achieved using the vanishing line of the measurement reference plane. We can obtain the vanishing line of the plane if we know at least two vanishing points on it. In order to get the vanishing points, we need two sets of parallel lines. The lines must be parallel to each other and parallel to the reference plane. The vanishing lines are defined by points that are marked manually. A minimum of three points must be marked on each line. Once the lines have been marked, the vanishing point is calculated through LSM as the vertex of the radiation that minimises the distance between marked points and radiation rays [16].

Once we have at least two vanishing points we form the vanishing line of the measurement reference plane. The parametric equation of the vanishing line can be written as:

$$\begin{pmatrix} x \\ y \end{pmatrix} = \lambda \begin{pmatrix} x_b - x_a \\ y_b - y_a \end{pmatrix} + \begin{pmatrix} x_a \\ y_a \end{pmatrix} \tag{8}$$

where $(x_a, y_a)^T$ and $(x_b, y_b)^T$ are the coordinates of the vanishing points. Using this vanishing line we can orient the image and make measurements on the reference plane. To orient the image, we must revert the effects of pan and tilt rotation since we are only interested in the distance measurement between points on the object and not its real orientation in the plane. Thus, for the rest of this study, we will assume that the swing rotation is null. Based on the vanishing line equation, the minimum distance from the principal point to vanishing line can be calculated as:

$$d = \frac{|x_a y_b - x_b y_a|}{\sqrt{(x_b - x_a)^2 + (y_b - y_a)^2}} \tag{9}$$

and the coordinates of the vanishing line point at this minimum distance are given by:

$$\begin{pmatrix} x_{\min} \\ y_{\min} \end{pmatrix} = \lambda^* \begin{pmatrix} x_b - x_a \\ y_b - y_a \end{pmatrix} + \begin{pmatrix} x_a \\ y_a \end{pmatrix} \tag{10}$$

with

$$\lambda^* = \frac{x_a \cdot (x_a - x_b) + y_a \cdot (y_a - y_b)}{\sqrt{(x_b - x_a)^2 + (y_b - y_a)^2}} \tag{11}$$

The new Y axis is placed perpendicular to the vanishing line by rotating through an angle α about z axis, where α is given by:

$$\alpha = \tan^{-1}\left(\frac{x_{min}}{y_{\min}}\right) \tag{12}$$

In this way, we undo the camera's pan rotation and, as a result, we get the image's new x axis is parallel to the object's X axis. In the absence of a camera tilt rotation, the x axis marks the horizontal vanishing line. When the vanishing line is parallel to the new x axis, we can undo the effect of tilt rotation with a rotation of the image coordinate system about the new x axis that fits the measurement plane's vanishing line with the x axis. As a result of this rotation, the image's new y axis is parallel to the object's Y axis. The rotation angle is given by:

$$\nu = \tan^{-1}\left(\frac{c}{d}\right) \tag{13}$$

where c is the focal length and d is the distance calculated according to Eq. (9).

2.2.2. Scale factor

With these two rotations we get a new coordinate system for the image with x and y axes parallel to object's X and Y axes, which makes it possible to make measurements on the reference plane if we have a proper scale factor. We get the proper scale factor of the plane using the information of the laser disto and it is mandatory that the laser pointer hits the measurement plane when the distance is about to be read. In order to get the scale factor, we need the image coordinates given by the distance meter. We can find these coordinates by direct observation of the image or by using a support model. The support model gives us the object coordinates of the distance meter laser pointer:

$$LP = \begin{pmatrix} X_{LP} \\ Y_{LP} \\ Z_{LP} \end{pmatrix} = \begin{pmatrix} X_L \\ Y_L \\ Z_L \end{pmatrix} + D \begin{pmatrix} V_X \\ V_Y \\ V_Z \end{pmatrix} \tag{14}$$

where D is the distance given by the distance meter. Using the collinearity condition [17], the image coordinates are:

$$lp = \begin{pmatrix} x_{LP} \\ y_{LP} \\ z_{LP} \end{pmatrix} = -c \begin{pmatrix} \frac{X_{LP}}{Z_{LP}} \\ \frac{Y_{LP}}{Z_{LP}} \\ 1 \end{pmatrix} \tag{15}$$

and by applying the rotations, we get the laser pointer coordinates in the new coordinate system, which is parallel to the object's plane system:

$$\begin{pmatrix} x'_{LP} \\ y'_{LP} \\ z'_{LP} \end{pmatrix} = R_\nu R_\alpha \begin{pmatrix} x_{LP} \\ y_{LP} \\ -c \end{pmatrix} \tag{16}$$

where R_α and R_ν are the angle rotation matrix about the z and x axes, respectively [18]. In [14], a single-point scale factor for a laser pointer is calculated. In order to use the scale factor with every point on the reference plane, we project the rotated point on an image reference plane in $z'=1$ prior to calculating the scale factor:

$$pl^* = \begin{pmatrix} x^*_{LP} \\ y^*_{LP} \\ 1 \end{pmatrix} = \begin{pmatrix} \frac{x'_{LP}}{z'_{LP}} \\ \frac{y'_{LP}}{z'_{LP}} \\ \frac{z'_{LP}}{z'_{LP}} \end{pmatrix} \tag{17}$$

The scale factor k is calculated as follows:

$$k = \frac{||LP||}{||lp^*||} = \frac{\sqrt{X_{LP}^2 + Y_{LP}^2 + Z_{LP}^2}}{\sqrt{1 + x_{LP}^{*2} + y_{LP}^{*2}}} \tag{18}$$

2.2.3. Object measurements

In order to make accurate measurements on the reference plane from 2-point image coordinates, two steps are necessary to find the oriented plane coordinates:

- Getting each point oriented coordinates by applying the rotations previously described:

$$\begin{pmatrix} x' \\ y' \\ z' \end{pmatrix} = R_\nu R_\alpha \begin{pmatrix} x \\ y \\ -c \end{pmatrix} \tag{19}$$

- Projecting points onto the image's coordinate system reference plane and applying the scale factor:

$$x = k \begin{pmatrix} x^* \\ y^* \\ z^* = 1 \end{pmatrix} = k \begin{pmatrix} \frac{x'}{z'} \\ \frac{y'}{z'} \\ \frac{z'}{z'} \end{pmatrix} \tag{20}$$

2.3. Measurement precision

In order to determine the quality of a measurement, we use an estimation of the precision of the coordinates of the points. In this work, we obtain a precision value from the propagation of the uncertainty of every single step in the image orientation and scaling process.

2.3.1. Vanishing point uncertainty calculation

As we have seen, a vanishing point calculation is based on the resolution of an over-determined system by using the least squares method. The main source of uncertainty in the vanishing point calculation comes from the location of the line points. Assuming that the precision of marking a line point is one pixel $\sigma_0^2 = 1$, we obtain the variance in the vanishing point A [1] as:

$$\sigma_A^{\,2} = \frac{\sum e_A^2}{m_A - n_A} \tag{21}$$

where e_A are the residuals of the points in the calculation of point A, m_A is the number of equations in the system that is solved to achieve the coordinates of the vanishing point A and n_A is the number of unknowns in the system. The variance–covariance matrix is:

$$\Sigma_A = \sigma_A^2 \begin{pmatrix} \sigma_{x_A}^2 & \sigma_{x_A y_A} \\ \sigma_{x_A y_A} & \sigma_{y_A}^2 \end{pmatrix} \tag{22}$$

where the values $\sigma_{x_A}^2$, $\sigma_{x_A y_A}$ and $\sigma_{y_A}^2$ are obtained from the inverse of the normal matrix of the system. Since the vanishing points A and B are independent, the covariance matrix of the vanishing points is given by:

$$\Sigma_{VP} = \begin{pmatrix} \Sigma_A & 0 \\ 0 & \Sigma_B \end{pmatrix} \tag{23}$$

2.3.2. Single image orientation uncertainty

The next step in the measurement calculation is the orientation and scaling of the image coordinates, so we can propagate the uncertainty in vanishing point calculation to the image orientation. Assuming that the camera and laser distance meter calibration errors are negligible, the uncertainty in image orientation and scaling mainly comes from the vanishing point location, although the scaling factor for the uncertainty depends on the support calibration as well. The uncertainty in the image's orientation is:

$$\Sigma_{OR} = J_{OR} \begin{pmatrix} \Sigma_{VP} & 0 \\ 0 & \Sigma_{\text{cal}} \end{pmatrix} J_{OR}^T \tag{24}$$

where

$$J_{OR} = \begin{pmatrix} \frac{\partial \alpha}{\partial x_A} & \frac{\partial \alpha}{\partial y_A} & \frac{\partial \alpha}{\partial x_B} & \frac{\partial \alpha}{\partial y_B} & 0 \\ \frac{\partial \nu}{\partial x_A} & \frac{\partial \nu}{\partial y_A} & \frac{\partial \nu}{\partial x_B} & \frac{\partial \nu}{\partial y_B} & 0 \\ \frac{\partial k}{\partial x_A} & \frac{\partial k}{\partial y_A} & \frac{\partial k}{\partial x_B} & \frac{\partial k}{\partial y_B} & J_{\text{cal}} \end{pmatrix} \tag{25}$$

is the Jacobian of the orientation angles and the scale factor, and

$$_{\text{Jcal}} = \begin{pmatrix} \frac{\partial k}{\partial X_L} & \frac{\partial k}{\partial Y_L} & \frac{\partial k}{\partial Z_L} & \frac{\partial k}{\partial V_X} & \frac{\partial k}{\partial V_Y} \end{pmatrix} \tag{26}$$

is the Jacobian of the scale factor dependence of the support calibration and Σ_{cal} is the variance–covariance matrix of the support calibration adjustment.

[1] We determine vanishing point B with analogous equations.

2.3.3. Oriented points uncertainty

The next step is calculating the oriented points through rotation angles and a scale factor. Since we are measuring points on a plane, the uncertainty of the X and Y coordinates depends on the orientation and scaling parameters as well as the marking point precision. Assuming that the marking point precision is one pixel, the precision in a single oriented point is:

$$\Sigma_P = J_P \begin{pmatrix} \Sigma_{OR} & 0 \\ 0 & I_2 \end{pmatrix} J_P^T \tag{27}$$

where $I_2 = \begin{pmatrix} 1 & 0 \\ 0 & 1 \end{pmatrix}$ is the 2×2 identity matrix and the Jacobian J_P is

$$J_P = \begin{pmatrix} \frac{\partial X}{\partial \alpha} & \frac{\partial X}{\partial \nu} & \frac{\partial X}{\partial k} & \frac{\partial X}{\partial x} & \frac{\partial X}{\partial y} \\ \frac{\partial Y}{\partial \alpha} & \frac{\partial Y}{\partial \nu} & \frac{\partial Y}{\partial k} & \frac{\partial Y}{\partial x} & \frac{\partial Y}{\partial y} \end{pmatrix} \tag{28}$$

2.3.4. Distance measurement

The last step is the computation of the distance between the coordinates of the two oriented points. The uncertainty in this step results from the uncertainty in the coordinates of the two points Σ_{P1} and Σ_{P2}. Thus, the uncertainty is:

$$\sigma_D = J_D \begin{pmatrix} \Sigma_{P1} & 0 \\ 0 & \Sigma_{P2} \end{pmatrix} J_D^T \tag{29}$$

where the Jacobian J_D is:

$$J_D = \begin{pmatrix} \frac{\partial D}{\partial X_1} & \frac{\partial D}{\partial Y_1} & \frac{\partial D}{\partial X_2} & \frac{\partial D}{\partial Y_2} \end{pmatrix} \tag{30}$$

The Jacobians are calculated using finite differences. The propagation of uncertainties makes it possible to estimate the measurement system's precision. This knowledge is important for system users, since knowing measurement precision makes it possible to check whether the measurement is suitable for a user's application or not.

3. Results

In order to test the system, two digital camera were used: a Canon EOS 10D with a 20 mm focal length lens and a Nikon D200 with a 20 mm lens. The distance meter was a Leyca Disto Plus with a precision of 1.5 mm. It is important to note that in this section a photograph or a shot not only refers to the photograph from the camera but the set of the photograph and the distance given by the distance meter.

3.1. Camera calibration

The camera was calibrated using the photogrammetric software Photomodeler. This process is based on a self-calibrating bundle adjustment. The calibration results and other camera parameters are shown in Table 1.

3.2. Support calibration

When testing a measurement system, some of the most important features are system repeatability and the time required for recalibration. In order to test the system repeatability, two kinds of tests were made. For the first test, the differences in the calibration parameters for different calibration sessions were taken into account. In the second test, we checked the setting and the resetting of two different support positions in the same calibration session. As a result, we found that the calibration parameters were within the 2-sigma confidence interval. Accordingly, it was necessary to make a calibration each time the system is used in order to get fine-tune the system and obtain accurate measurements. The calibration results are given in Table 2. This data shows the calibration parameters for the setting and resetting test with distance meter's laser beam close to parallel to optical axis.

By calibrating the support, we can establish a relationship between the image coordinates and the distance given by the laser distance meter. This permits us to obtain a scale factor between the object-space reference plane and the image-space reference plane. Calibrating the support also makes it possible to obtain the distance meter's laser pointer coordinates in the object and image spaces, given respectively by Eqs. (14) and (15). Since the relative orientation between the laser disto and digital camera is known by calibration, the coordinates of the laser pointer lie on a straight line that fits the laser beam of the disto and which is independent of the captured scene. This relationship is very important because it can be very hard to visually detect the laser pointer in the image. The visibility of the laser pointer depends not only on the distance of the reference plane but on the lighting conditions and the reflectivity of the reference surface. We can see that the precision of the laser pointer varies with distance. The precision is higher for longer distances because the support calibration only weakly depends on the distance: given that the angular uncertainty of the support calibration is very small, the uncertainty of the laser pointer's object coordinates, given by Eq. (14), increases slowly with distance; therefore, the uncertainty of laser pointer image coordinates, given by Eq. (15), decreases with distance. This precision marks the operational distances for using the support calibration instead of visual detection to get the laser pointer image coordinates. At closer distances, when the precision is worse, the laser pointer is easier to visually detect in the image. On the contrary, support precision is higher at longer distances when laser pointer is hardly detected.

3.3. Measurement process

In order to test the accuracy of the measurement process, a large number of photographs with different orientations were taken and divided in two groups depending on the distance from the system to the reference plane. We made several measurements with this photographs and compare the results with the validation measurements in order to obtain the measurement errors.

The first group includes short-distance photographs. A set of 60 photographs from 5 different scenes where taken all of them containing enough parallel lines for orientation. An approximate number of 600 measurements were made in this setup. The validation measurements were made with a measurement tape. In this group, the objects to be measured fill the most of the photograph. These photographs can be

Table 1
Camera calibration. Camera calibration parameters for Canon EOS10D and Nikon D200.

	Canon Eos 10 D	Nikon D200
Focal length	20.973218 mm	20.742753 mm
Principal point	(11.179244, 7.500561) mm	(11.877440, 8.174458) mm
Sensor format	(22.670730, 15.113000) mm	(23.900010, 16.000000) mm
Radial distortion: K1	1.938e-004	2.692e-004
Radial distortion: K2	−2.058e-007	−4.093e-007
CCD resolution	3072×2048	3872×2592

Table 2
Support repeatability. Three calibration results for parallel settings.

	Calibration 1	Calibration 2	Calibration 3
X_L (m)	−0.2038± 0.0011	−0.2055± 0.0012	−0.2053± 0.0011
Y_L (m)	−0.0059± 0.0004	−0.0063± 0.0003	−0.0064± 0.0003
Z_L (m)	0.1524±0.0050	0.1509± 0.0055	0.1512± 0.0052
V_X (rad)	−0.0133±0.0001	−0.0144±0.0001	−0.0114± 0.0002
V_Y (rad)	−0.0424± 0.0001	−0.0424±0.0001	−0.0422± 0.0001
V_Z (rad)	−0.9990± 0.0001	−0.9989±0.0001	−0.9990±0.0002

Table 3
Mean and standard deviation in tests.

	Set 1: Short distance			Set 2: Long distance		
	Precision (m)	Abs. error (m)	Rel. error	Precision (m)	Abs. error (m)	Rel. error
Mean	0.003	0.005	0.9%	0.013	0.015	0.5%
Std dev		0.004	0.9%		0.022	0.5%

used to measure constructive elements like door and window openings in indoor scenes. In this short-distance photographs, the laser pointer is usually easier to detect in the image and the spatial resolution is high. On the other hand, the indoor lighting conditions can be very challenging for backlit images and it is difficult to have two different sets of parallel lines depending on the photograph.

The second group includes shots at longer distances that make it possible to measure façades. A set of 90 photographs corresponding to 6 different façades were taken, having more than 1100 measurements in this setup. The validation measurements of this group were made with a laser-total station on the façades. Due to the difficulty in making corner measurements with a laser-total station, the validation measurements of the façades were made at points of interest easily distinguishable on the surface of the façade. Each measurement was repeated three times in order to have better precision in the total station measurements. Long-distance photograph characteristics are just the opposite of short-distance: laser detection is difficult, there is a lower spatial resolution and parallel lines of orientation are easier to find, especially for wide angle lenses.

Once we discard the outliers of the measurements, the available number of measurements for the accuracy assessment of the system is more than 1500.

3.4. Error results

All of the tests carried out to evaluate the acuraccy of our system were performed using a software created using C# and XML. This software allowed us to configure the measurement system by setting the calibration parameters of both the camera and support. The user can introduce several images to the measurement project and the images are processed independently. Then, each image is manually marked for orientation and measurement purposes. To do so, the user has to set the number of parallel lines for the two sets of lines in order to orient the image, where each line is marked by at least three points. After the image is oriented, the software computes the distance and precision between two consecutive measurement points and exports the results to a spreadsheet or a PDF file. In Fig. 4 we can see a snapshot of the developed software lines marked (left) and the vanishing line obtained for image orientation (right). In the first group of tests (short-distance tests), the maximum distance of the shot was 10 m. The mean of the precision calculated according to (29) was 3 mm. The absolute mean error of these tests was 5 mm and about 95% of the absolute error values were lower than 11 mm. The relative mean error was 0.9% and more than 95% of the values were lower than 3%.

For the second group of tests the distance of the shot was between 10 and 40 m. The mean of the precision was 13 mm and the absolute mean error of these tests was 15 mm for the absolute error and 0.5% for the relative error. For the 95% error values, the result was 50 mm for the absolute error values and lower than 1.5% for the relative errors.

The absolute error is lower in short-distance measurements because the spatial resolution of the photograph is higher at short distances and objects' dimensions are smaller. On the contrary, the relative errors of the short-distance measurements were almost twice the size of the relative errors of the long-distance measurements.

The maximum measurement distance between points was of 2.242 m for the short-distance tests and 16.709 m for the long-distance tests; therefore, higher relative errors were expected for the short-distance tests. In both cases, we removed measurement outliers when calculating the error. Table 3 shows mean and standard deviation values for the absolute and relative errors and the precisions of both test sets. The relative error histogrammes for both tests are shown in Fig. 5.

For the whole of the measured distances, it is satisfied that

$$\frac{E}{\sigma_D} \sim N(\mu, \sigma)$$

where E is the error in the measurement and σ_D is the estimation of the uncertainty in the measured distance. The estimated parameters of the normal distribution resulted to be $\bar{x} = 0.04$ and $s = 1.326$ The confidence intervals for mean, when the sample size is large, and standard deviation are given by

$$I_\mu = \left[\bar{x} - z_{\frac{\alpha}{2}}\frac{s}{\sqrt{n}}\ \bar{x};\ + z_{\frac{\alpha}{2}}\frac{s}{\sqrt{n}}\right] \tag{31}$$

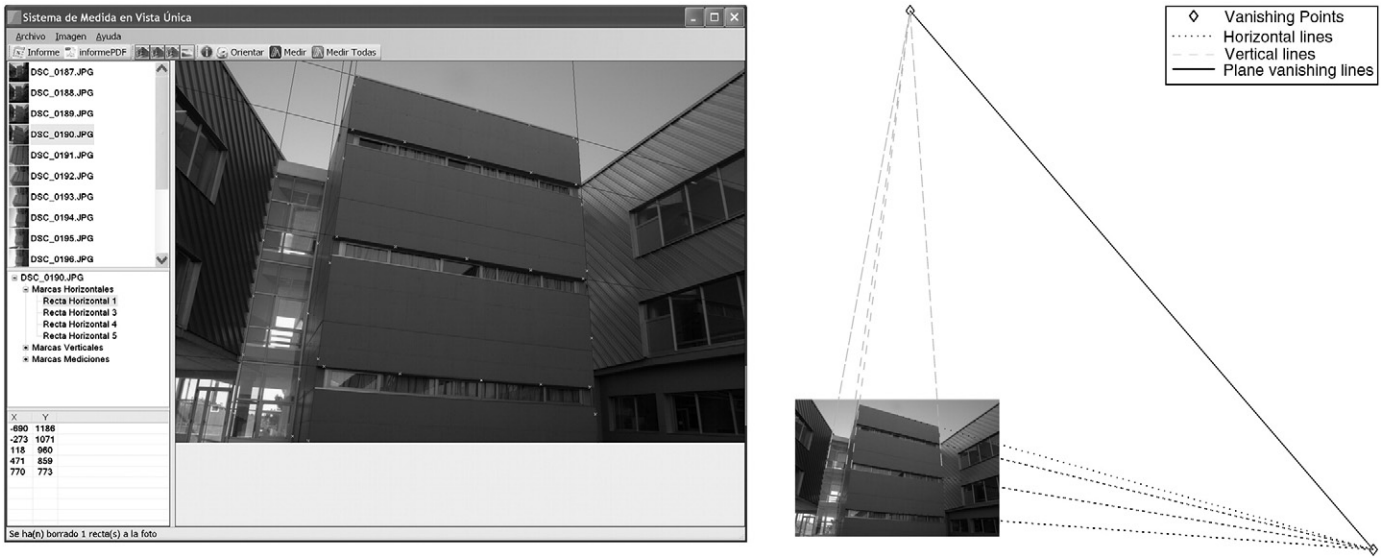

Fig. 4. Developed software for façade measurement (left) and computed vanishing line for orientation (right).

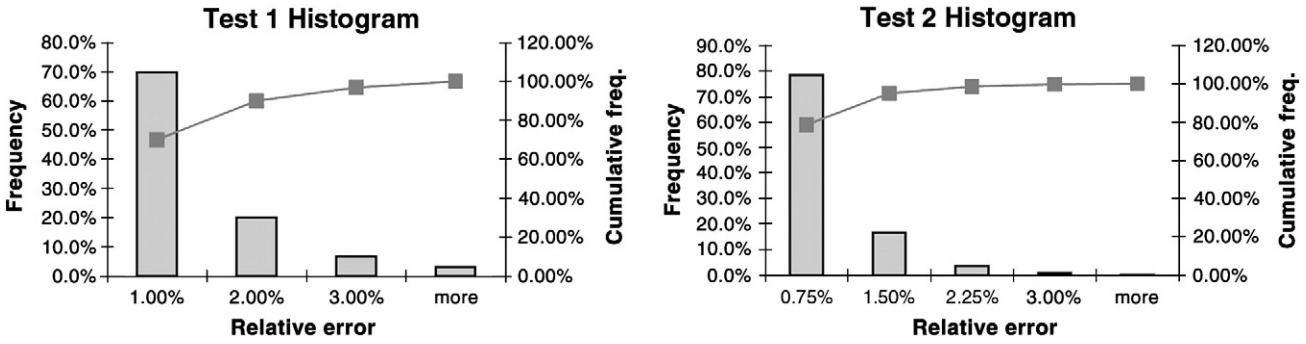

Fig. 5. Relative error histograms and cumulative frequency distribution for test at short distances (left) and long distances (right).

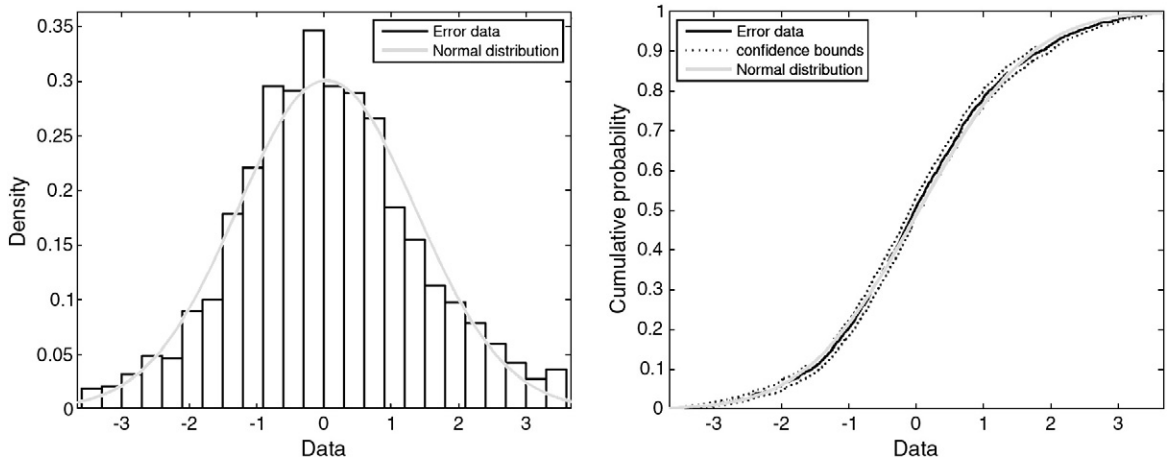

Fig. 6. Histogram of error/precision quotient and normal density function fitted to the data (left). Cumulative distribution function of data with corresponding confidence bounds and fitted normal cumulative distribution (right).

and

$$I_\sigma = \left[\sqrt{\frac{(n-1)s^2}{\chi^2_{\alpha/2}}}; \sqrt{\frac{(n-1)s^2}{\chi^2_{1-\alpha/2}}} \right] \tag{32}$$

respectively, where $z_{\infty/2}$ is the value of a random variable having the standard normal distribution, $\chi^2_{\alpha/2}$ is the value of a random variable having a chi-square distribution, $(1-\alpha)$ is the confidence level and n is the sample size[19]. Particularizing for our data, the confidence intervals for mean and stardard deviation are respectively $I_\mu = [-0.025; 0.1064]$ and $I_\sigma = [1.281;\ 1.374]$. Fig. 6 shows the fit of the error data to the normal distribution.

The number of samples that ensure a confidence interval I for the mean μ is given by [19]:

$$n^* = \left(\frac{z_{\alpha/2}\sigma}{I}\right)^2 (\text{for large } n) \tag{33}$$

Then, considering a confidence level of 95%, we could have a confidence interval as small as $I = 0.05\sigma$, since the sample size for that interval would be $n^* = \left(\frac{1.96}{0.05}\right)^2 \approx 1537$ samples and our sample size is 1569 data.

Given that the $\frac{|E|}{\sigma_D}$ quotient above follows a normal distribution, 95% of the values are inside the interval $[-1.96\sigma;\ 1.96\sigma]$ Using this results, we obtain limits for the quotient $\frac{|E|}{\sigma_D}$ for a 95% confidence level of 2.60.

4. Conclusions

In this work, we analysed the precision and accuracy of a planar-surface measurement system based on close-range photogrammetry. The system was initially used to measure façades, but other applications are possible as well. Several tests were made on building façades and grouped in two test sets depending on the distance to the camera, since it is possible to measure single windows or a whole façade by varying this distance. For large distances, several parallel lines can be used to orient the image, which increases the accuracy of the measurement, but sometimes the object to be measured only fills a small area on the image, which negatively affects the accuracy. For the opposite is true for small distances.

We have seen that the support calibration is stable, but repeatability tests showed that it is necessary to recalibrate the system in order to get accurate measurements. This system allows for different relative positions between the digital camera and the laser distance meter. This is useful for small distances in indoor environment measurements where it can be difficult to locate the distance meter laser pointer on the reference plane; this feature is limited by the repeatability of the support calibration. For large distances (more than 10 m), there is no need to change the relative position of the support since it is possible to place the laser pointer on the reference plane by changing the tripod's orientation.

Since the real measurements of the objects are unknown, the measurement precision can be calculated via the uncertainties of the vanishing points. The accuracy of single-image measurements with this measuring system is less than 11 mm (for 95% of the values) for the short-distance tests and less than 50 mm (for 95% of the values) for longer distances.

References

[1] F.A. Van Den Heuvel, 3D reconstruction from a single image using geometric constraints, ISPRS Journal of Photogrammetry and Remote Sensing 53 (6) (1998) 354–368.

[2] F.A. Van Den Heuvel, Exterior Orientation using Coplanar Parallel Lines, in:, 10th Scandinavian Conference on Image Analysis, Lappeenranta, 1997, pp. 71–78.

[3] A.M.G. Tommaselli, M.L.L. Reiss, A photogrammetric method for single image orientation and measurement, Photogrammetric engineering and remote sensing 71 (6) (2005) 727–732.

[4] P.F. Sturm, S.J. Maybank, A Method for Interactive 3D Reconstruction of Piecewise Planar Objects from Single Images, In: Proc. British Machine Vision Conference, 1999, pp. 265–274.

[5] B. Caprile, V. Torre, Using vanishing points for camera calibration, International Journal of Computer Vision 4 (2) (1990) 127–139.

[6] R. Cipolla, T. Drummond, D. Robertson, Camera Calibration From Vanishing Points in Images of Architectural Scenes. In Proc. British Machine Vision Conference, 1999.

[7] F.A. Van Den Heuvel, Vanishing Point Detection For Architectural Photogrammetry, Proc. European Conference of Computer Vision Springer, 1998, pp. 652–659.

[8] D.G. Aguilera, J. Gomez-Lahoz, J. Finat, A New Method for Vanishing Points Detection in 3D Reconstruction from a Single View, The Intl. Archives of the Photogrammetry , Remote Sensing and Spatial Information Sciences, XXXVI, 2005.

[9] C. Bräuer-Burchardt, K. Voss, Robust vanishing point determination in noisy images, International Conference on Pattern Recognition 1 (2000) 1559.

[10] C. Bräuer-Burchardt, K. Voss, Façade reconstruction of destroyed buildings using historical photographs, Proc. 19 th International Committee for Documentation of Cultural Heritage (CIPA) Int. Symp., Potsdam, 2001, pp. 543–550.

[11] G.E. Karras, E. Petsa, Metric Information from Uncalibrated Single Images, In: Proceedings of the XVII International Committee for Documentation of Cultural Heritage (CIPA) Symposium, Olinda/Brasil (available in CD), 1999.

[12] A. Criminisi, I.D. Reid, A. Zisserman, A Plane Measuring Device, Proc. British Machine Vision Conference, 1997.

[13] A. Criminisi, I. Reid, A. Zisserman, Single view metrology, IEEE International Conference on Computer Vision 1 (1999) 434.

[14] C. Ordonez, P. Arias, J. Herraez, J. Rodriguez, M. Martin, A combined single range and single image device for low-cost measurement of building façade features, The Photogrammetric Record 23 (122) (2008) 228–240.

[15] Eos Systems. www.photomodeler.com. 2009.

[16] R. Hartley, A. Zisserman, Multiple View Geometry in Computer Vision, Cambridge University Press, New York, NY, USA, 2000.

[17] K. Kraus, Photogrammetry, vol. 1, Fundamentals and standard processes, Dümmler Verlag, Bonn, 2000.

[18] K. Kraus, Photogrammetry, vol. 2, Advanced Methods and Applications, Dümmler Verlag, Bonn, 2000.

[19] B. Ayyub, Probability, Statistics, and Reliability for Engineers and Scientists 2ed, Chapman & Hall/CRC Press, Florida, 2003.